Do Evanescent Modes Violate Relativistic Causality?

G. Nimtz

II. Physikalisches Institut, Universität zu Köln, Zülpicher Str. 77, 50937 Köln, Germany
G.Nimtz@uni-koeln.de

Abstract. Time dependent experiments with evanescent modes (photonic tunneling) can be performed with high precision and at a macroscopic scale with microwaves in the range of meters or in the infrared regime in the range of centimeters. The infrared technology is the present day digital signal processing and transmission. Superluminal (faster than light) signal transmission by evanescent modes was shown by Enders and Nimtz already 1992 [1].

Evanescent modes are solutions of the Helmholtz equation with imaginary wave vectors which are equivalent to the tunneling solutions of the Schrödinger equation. Experiments of transmission and of partial reflection of microwaves by photonic potential barriers revealed superluminal signal velocity of evanescent modes. The effect is a near field phenomenon and violates the relativistic causality.

In this contribution superluminal experiments are introduced and explained.

1 Introduction

During the last decade much research and arguing was devoted to superluminal signal velocity $v_{\text{signal}} > c$, where c is the vacuum velocity of light [2–5]. I am not talking about the phase velocity $\mathbf{v}_{\text{phase}}$, which exceeds in several media the velocity c of light. The relevant *signal velocity* is in charge of the transmission of a *defined cause and subsequent effect*. Actually, the near field phenomena evanescent modes and tunneling represent the exception of $v_{\text{signal}} \leq c$.

In this lecture I present experiments on superluminal signal velocity of evanescent modes. Evanescent modes are solutions of the Helmholtz equation. Like wave mechanical tunneling functions these special solutions are characterized by a purely imaginary wave number. The wave number represents 2π times the reciprocal wavelength. Accordingly evanescent modes do not have a real wave length and the phase time approach conjectured the observed instantaneous field spreading of evanescent modes. However, a superluminal signal velocity does not violate the *primitive causality* (the effect cannot precede the cause). But a superluminal signal velocity violates the *relativistic causality*, often called Einstein causality: no signal can propagate with a velocity greater than c. *Experiments*

G. Nimtz: *Do Evanescent Modes violate Relativistic Causality?*, Lect. Notes Phys. **702**, 506–531 (2006)
DOI 10.1007/3-540-34523-X_19

show that detectors receive signals transmitted by evanescent modes earlier than signals, which traveled the same distance in vacuum. For instance the detector makes earlier click in the case of a tunneled digital signal or receives a tunneled melody before detecting the air born one. Even though as explained in Sect. 8 the design of a time machine is still not possible by signaling with superluminal evanescent modes.

Studies with evanescent waves were stimulated in order to obtain analogous experimental data on quantum mechanical tunneling time. Tunneling represents the quantum mechanical analogy to the electromagnetic evanescent modes [6]. As there have been no experimental data on quantum mechanical tunneling time available, the propagation time of evanescent modes was studied, which is easier to measure than particle tunneling time. More over in the case of electron tunneling in semiconductor devices there are present time consuming parasitical Coulomb interactions which determine the measured tunneling time.

The tunneling time is of the order of the reciprocal frequency of the wave packet [13, 15]. This time is spent at the entrance boundary as will be shown in Sect. 6. From an experimental point of view the transit time for a wave packet propagating through a barrier is measured as the interval between the arrivals of the signal envelope at the two ends of that region.

An example of evanescent digital signals transmitted with microwaves is displayed in Fig. 1. The half width (the time duration at half the maximum intensity) represents the number of digits. To make a comparison the small tunneled wave packet is amplified by about a factor of 10 000 (i.e. 40 dB), however, re-

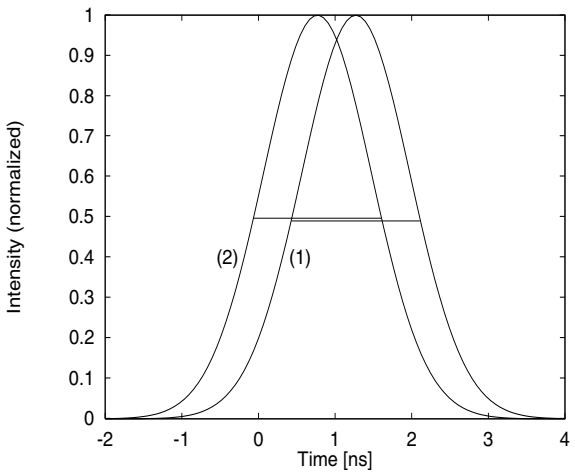

Fig. 1. Intensity vs time of a microwave pulse (2), which has tunneled at superluminal velocity through a photonic barrier in a wave-guide of 114.2 mm length. For comparison the tunneled, digital signal is normalized with a pulse (1), which propagated through a normal waveguide of the same length. The tunneled digital signal traveled at a speed of $4.7\,c$ [7]. The halfwidth (*solid line*) of the pulse equals the number of digits, i.e. it represents the signal

member that a signal is independent of intensity as its intensity exceeds that of the thermal noise as discussed in Sect. 7. The evanescent pulse displayed in Fig. 1 traveled with a superluminal velocity of $4.7\,c$.

Incidentally, $v_{\rm signal} > c$ does not occur in experiments based on a near to resonance interaction with a Lorentz–Lorenz like oscillator. This oscillator is the paradigm of particle polarization in electric fields [8]. In those experiments pulses can display even a negative group velocity [9]. But only the peak of the pulse traveled at a negative group velocity and not the whole envelope of the signal. The interacting field distribution of the signal was reshaped and the signal envelope traveled at subluminal velocity.

At present there is much ado about quantum teleportation [10]. As those sophisticated quantum mechanical experiments include a classical communication channel the signal velocity becomes $v_{\rm signal} \leq c$ finally. Incidentally, teleportation is a technique applied in telecommunication for a long time, where sound (phonons) are transformed into electromagnetic waves (photons), which travel a million times faster than sound and the receiver transformed the electromagnetic waves back into the slow but understandable sound. For the time being evanescent modes and tunneling seem to represent the only mechanisms to achieve superluminal signal velocities.

In the following some elementary quantities and relations are reminded. The propagation of waves $\psi \sim e^{i(\mathbf{k}\cdot\mathbf{x}-\omega t)}$ in space is described by the a relation connecting the wave number $\mathbf{k}$ or, equivalently, the wavelength with the angular frequency ω

$$k = k(\omega) = k_0 \cdot n(\omega)\,, \qquad \lambda(n) = \lambda_0/n(\omega)\,. \tag{1}$$

Here k_0 is the wave number and λ_0 the wavelength of waves in vacuum which are related $k_0 = 2\pi/\lambda_0$. Furthermore, $n(\omega) = n'(\omega) - in''(\omega)$ is the refractive index n we are familiar with from Snellius' law. The quantities n' and n'' real and imaginary parts of the refractive index of the medium in question. Both quantities, k and n are in general complex functions of frequency. The imaginary parts describe the attenuation or amplification of waves. The attenuation may be caused either by dissipation or by reflection. Waves with purely imaginary refractive index $n(\omega)$ and wave number $k(n)$ are called *evanescent modes*.

2 Wave Propagation

2.1 Maxwell and Schrödinger Equations

For electromagnetic waves and hence for photons, the propagation of waves can be described by the Maxwell equations and for massive particles by the Klein–Gorden, the Dirac or, in the non-relativistic regime, by the Schrödinger equation.

The Maxwell equations in media characterized by some refractive index $n = \sqrt{\mu\epsilon}$, where μ and ϵ are the relative permeability and the relative permittivity, lead to the wave equation

$$-\nabla^2\phi(\mathbf{x},t) + \frac{n^2}{c^2}\frac{\partial^2}{\partial t^2}\phi(\mathbf{x},t) = 0\,, \tag{2}$$

ϕ being any component of the electrical and the magnetic fields. In vacuum characterized by $n = 1$ waves propagates with the velocity $c = (\mu_0\epsilon_0)^{-1/2}$, where μ_0 and ϵ_0 are the permeability and the permittivity, respectively.

If we describe phenomena periodic in time with frequency $\nu = \omega/(2\pi)$,

$$\phi(\mathbf{x}, t) = \phi_x(\mathbf{x})e^{i\omega t}\,, \tag{3}$$

then the wave equation reduces to the Helmholtz equation

$$\nabla^2\phi_x(\mathbf{x}) + \frac{n^2\omega^2}{c^2}\phi_x(\mathbf{x}) = 0\,. \tag{4}$$

As usual, this equation will be solved by a plane wave ansatz

$$\phi_x(\mathbf{x}) = \phi_0 e^{-i\mathbf{k}\cdot\mathbf{x}}\,, \tag{5}$$

what leads to a relation between the wave number and the refractive index

$$k^2 = \frac{n^2\omega^2}{c^2} = k_0^2 n^2 = k_0^2\epsilon\mu\,, \tag{6}$$

where k_0 is the wave number in free space. If k and, thus, n are purely imaginary then the solution is called an *evanescent mode*. The imaginary wave number is usually expressed by κ. In Sect. 3 we will discuss three popular examples, where these special solutions occur.

Similar features can be found for the stationary Schrödinger equation

$$E\psi(\mathbf{x}) = -\frac{\hbar^2}{2m}\nabla^2\psi(\mathbf{x}) + U(\mathbf{x})\psi(\mathbf{x})\,, \tag{7}$$

where E is the energy of the stationary state, m is the mass of the particle and $U(\mathbf{x})$ is a position-dependent potential, the barrier potential, for example. This relation is mathematically equivalent to the Helmholtz equation

$$\nabla^2\psi(\mathbf{x}) + \frac{2m}{\hbar^2}(E - U(\mathbf{x}))\psi(\mathbf{x}) = 0\,. \tag{8}$$

Again, a plane wave ansatz

$$\psi(\mathbf{x}) = \psi_0 e^{-i\mathbf{k}\cdot\mathbf{x}} \tag{9}$$

yields for the wave number k

$$k^2 = \frac{2m}{\hbar^2}(E - U) = k_0^2 - \frac{2mU}{\hbar^2}\,, \tag{10}$$

where $k_0^2 = 2mE/\hbar^2$ is the wave vector at infinity, where U is assumed to vanish. Particles in regions for which $E < U$, that is, inside the potential barrier, are quantum analogues of evanescent modes. Obviously, for the electromagnetic evanescent modes the refractive index plays the role of the potential in the wave mechanical tunneling.

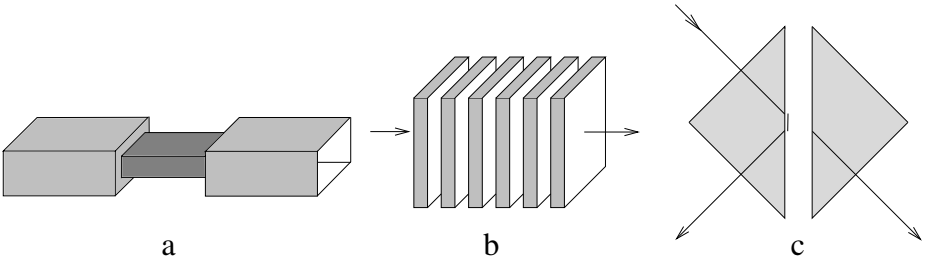

Fig. 2. Sketch of three photonic barriers. (**a**) illustrates an undersized wave guide (the central part of the wave guide has a cross section being smaller than half the wavelength in both directions perpendicular to propagation), (**b**) a 1-dimensional photonic lattice (periodic dielectric hetero structure), and (**c**) the frustrated total internal reflection of a double prism, where total reflection takes place at the boundary from a denser (the first prism with refractive index n_1) to a lesser dielectric medium (with refractive index n_2)

3 Photonic Barriers, Examples of Evanescent Modes

Prominent examples of evanescent modes are found in undersized wave guides (both dimensions of the guide cross section are smaller than half the vacuum wavelength), in the forbidden frequency bands of periodic dielectric hetero-structures (photonic lattice), and with double prisms in the case of frustrated total internal reflection [3,5]. The three examples are illustrated in Fig. 2. Dielectric lattices are analogous to electronic lattices of semiconductors with forbidden energy gaps. As seen below the square number of the imaginary refractive index n''^2 corresponds to a negative effective potential $E-U$ in the Schrödinger equation. Each of the three barriers introduced in Fig. 2 have a different dispersion relation of the wave number $k(\omega)$, of the refractive index $n(\omega)$, and then of the transmissivity $T(\omega)$.

3.1 Undersized Waveguide

Figure 2a displays an undersized waveguide with the long side a of the waveguide cross section which is mounted between two properly sized parts. From the wave equation (2) one can easily determine the wave vector

$$k = k_0\sqrt{1-\left(\frac{\lambda_0}{\lambda_{\text{cutoff}}}\right)^2} = k_0\sqrt{1-\left(\frac{\omega_{\text{cutoff}}}{\omega_0}\right)^2} = k_0 n(\omega)\,, \qquad (11)$$

where we introduced the cutoff wavelength $\lambda_{\text{cutoff}} = 2a$ which is related to the angular cutoff frequency $\omega_{\text{cutoff}} = \pi c/a$. Below the cutoff frequency or above the cutoff wavelength the waveguide wave propagation is prohibited since in that case the wave number $n(\omega)$ becomes imaginary. Then the solution represents an evanescent mode. The intensity of this evanescent mode decreases by $1/e$ at a distance a/π: The field does not propagate and dies off rapidly with distance.

3.2 Photonic Lattice

The photonic lattice of Fig. 2b represents a one-dimensional analogue of the electronic lattice we are familiar with from semiconductor physics. Under Bragg condition an infinite lattice displays total reflection. Such photonic mirrors are frequently used in photonics and semiconductor lasers. They are specified by a higher reflectivity than metallic mirrors.

An incoming electromagnetic wave $\mathbf{E}^{\text{in}}$ will be partially reflected and partially transmitted by a finite barrier. The ratio between reflected and incoming wave defines the reflection coefficient $r = E_n^{\text{reflected}}/E_n^{\text{in}}$ and the ratio between the transmitted wave and the incoming wave the transmission coefficient $t = E_n^{\text{trans}}/E_n^{\text{in}}$ where E_n denotes the normal component of the vector $\mathbf{E}$. In general, the transmission and reflection coefficients t and r are complex

$$t = \sqrt{T}e^{i\varphi_t} \tag{12}$$

$$r = \sqrt{R}e^{i\varphi_r}, \tag{13}$$

where the transmissivity $T = |t|^2$ and the reflectivity $R = |r|^2$. They are related due to conservation of energy as

$$T + R = 1\,. \tag{14}$$

The one-dimensional lattice introduced and studied here is built up by layers with a periodic alteration of the refractive index. The elementary cell is given by the two quarter wave length layers of thicknesses d_1 and d_2

$$n_1 d_1 = n_2 d_2 = \lambda_0/4 \tag{15}$$

$$\omega_0 = 2\pi c/\lambda_0, \tag{16}$$

where ω_0 corresponds to the mid-gap angular frequency of such an arrangement. The mid-gap frequency is given by the resonance condition (15) and is displayed as transmission minimum in Fig. 3. (Fig. 3 shows the transmission gaps of two structures and Fig. 9b displays the frequency spectrum of a signal displaced in the middle of the forbidden frequency gap.) Next I will calculate the transmission function for the quarter-wavelength unit cell. The transmission coefficient as defined above can be given by the complex number

$$t = \sqrt{T}e^{i\varphi_t} \tag{17}$$

The transmission for the quarter wave stack is

$$t = \frac{T_{12}e^{i(p+q)}}{1 - R_{12}e^{2iq}}, \tag{18}$$

where

$$T_{12} = t_{12}t_{21} = \frac{4n_1n_2}{(n_1 + n_2)^2}, \tag{19}$$

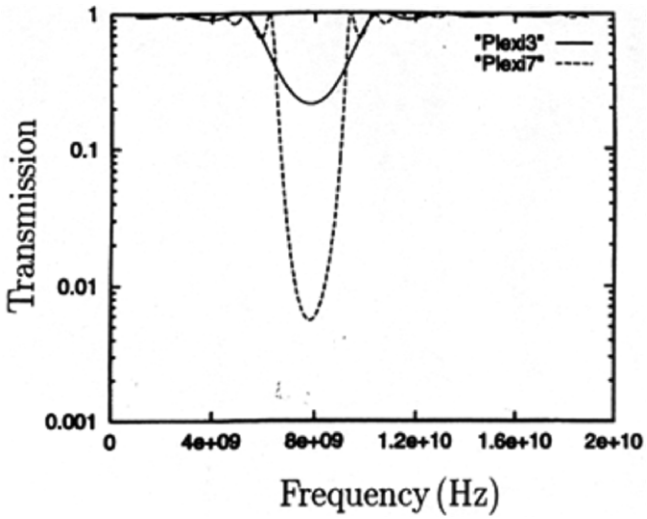

Fig. 3. Transmissivity T as a function of frequency of periodic dielectric quarter-wavelengths structures with 7 and with 3 perspex layers, respectively. The interference pattern shows small minima due to multiple layer destructive interference

and

$$R_{12} = r_{12}^2 = \left(\frac{n_1 - n_2}{n_1 + n_2}\right)^2 , \tag{20}$$

are the double-transmission and reflection factors. Here, $p = n_1 d_1 \omega/c$ and $q = n_2 d_2 \omega/c$, where 15 holds in addition for a quarter wave stack. After extracting the real and the imaginary parts from the quarter cell transmission coefficient, $t^{\lambda/4}$, we have unit-cell expressions for $x^{\lambda/4}$ and $y^{\lambda/4}$,

$$x^{\lambda/4} = T_{12} \frac{\cos(\pi\omega') - R_{12}}{1 - 2R_{12}\cos(\pi\omega') + R_{12}^2} , \tag{21}$$

$$y^{\lambda/4} = T_{12} \frac{\sin(\pi\omega')}{1 - 2R_{12}\cos(\pi\omega') + R_{12}^2} , \tag{22}$$

$$T^{\lambda/4} = \frac{T_{12}^2}{1 - 2R_{12}cos(\pi\omega') + R_{12}^2} , \tag{23}$$

where $\omega' = \omega/\omega_0$.

The extension of the relations for an $N = 1$ stack to N an arbitrary number of stacks is presented in Refs. [13, 14], for example.

Numerical data for 3 and 7 stacks are displayed in Figs. 3; 4; 5. Figs. 3–7 illustrate the transmission, the phase shift, and the group velocity as a function of frequency of a photonic lattice in the microwave frequency regime. The data are in agreement with the experiments [3, 5]. The lattice has either 7 or 3 quarter-wavelength perspex layers, which are separated by quarter-wavelength air distances (in this example the refractive indices are $n_1 = 1.6$ and $n_2 = 1.0$)

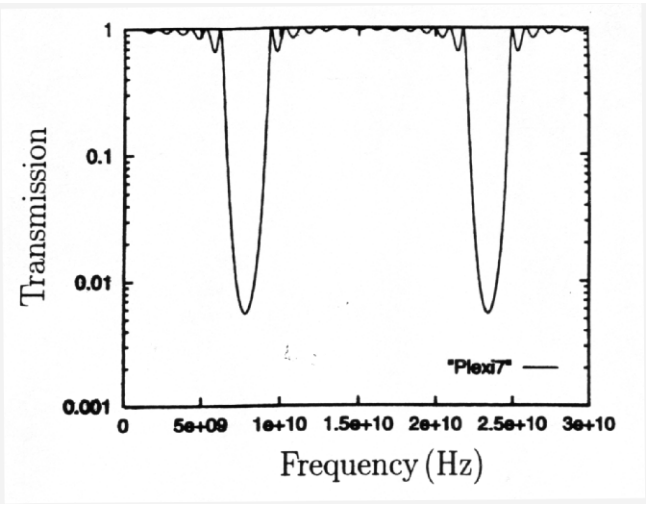

Fig. 4. The transmissivity displays two forbidden band gaps in this frequency range between 0 and 30 GHz. Gaps appear periodically in frequency, in this graph by about 8 and 24 GHz. The data shown is valid for $N = 7$ layers

Figure 5 displays for both structures a reduced phase derivative in the forbidden evanescent frequency regime. *This very derivative equals the above mentioned scattering phase shift and equivalently the scattering time at the barrier front boundary.* The phase time approach is made plausible in Sect. 5.2

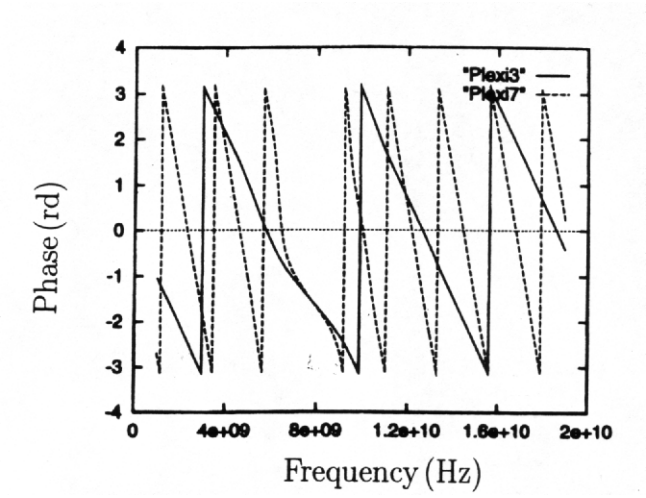

Fig. 5. Phase vs frequency of the lattice. The small phase shift in the evanescent regime of the lattice is due to the phase shift at the barrier front boundary. Inside the barrier the phase shift is zero in consequence of the imaginary wave number

Calculated and measured spectra of the transmission of an infrared periodic dielectric hetero-structure are shown in Fig. 9b.

3.3 Frustrated Total Internal Reflection: The Double Prisms

Double prisms are subject of research since Newton. He already conjectured the Goos-Hänchen shift. This non-specular reflection effect was measured only in 1947. A hundred years ago J. C. Bose studied the transmission of radio wave intensity, i.e. tunneling depending on the gap length [20]. The following dispersion relation describes the frustrated total internal reflection (FTIR) of double prisms. In the case of double prisms the total reflection is called frustrated since a small amount of the incident beam is tunneling into the second prism as sketched in Fig. 2c. In the case of FTIR the imaginary wave number κ in the barrier region and the tunneled electric field E_t measurable outside the barrier are given by the relations [6]

$$\kappa = \frac{\omega}{c}\sqrt{\frac{n_1^2}{n_2^2}\sin^2\theta - 1}\,, \tag{24}$$

$$E_t = E_0(x)e^{i\omega t - \kappa x}, \tag{25}$$

where θ is the angle of the incident beam (larger than the angle of total reflection), $E(x = 0)$ the amplitude of the electric field at the barrier front, n_1 and n_2 are the refractive indexes, and $(n_1/n_2)\sin\theta > 1$ holds in the case of total reflection. ω is the angular frequency, t the time, x the distance of the prisms, and κ the imaginary wave number of the tunneling mode. *Incidentally, n_1 and n_2 do not represent the effective refractive index of the evanescent mode traversing the gap between the prisms, the latter being imaginary.*

Equation (24) is derived from reflection of a beam at the surface of a medium with refractive index n_2. The incident beam comes from a material with a real index n_1 greater than n_2 under the angle θ_i. Snell's law says that

$$n_1 \sin\theta_i = n_2 \sin\theta_t. \tag{26}$$

The angle θ_t of the transmitted wave becomes 90^0 when the incident angle θ_i is equal to the critical angle θ_c given by

$$\frac{n_1}{n_2}\sin\theta_c = 1. \tag{27}$$

The magnitudes of the wave vectors, that is, of the incident wave number $\boldsymbol{k}$, of the reflected wave vector $\boldsymbol{k}_r$, of the transmitted wave vector $\boldsymbol{k}_t$, the wave vector parallel $\boldsymbol{k}_\parallel$ and perpendicular $\boldsymbol{k}_\perp$ to the boundary follows from the boundary conditions at the interface. They are given by

$$k^2 = n^2\omega^2/c^2 \tag{28}$$
$$k_t^2/n_2^2 = k_r^2/n_1^2 = k^2/n_1^2 \tag{29}$$
$$k_{t,\parallel} = k_{r,\parallel} = k_\parallel \tag{30}$$
$$k_{r,\perp}^2 + k_{r,\parallel}^2 = k_\perp^2 + k_\parallel^2 \tag{31}$$
$$k_{r,\perp}^2 = k_\perp^2 \tag{32}$$
$$k_{r,\perp} = -k_\perp\,. \tag{33}$$

With $k_t^2 = k_{t,\parallel}^2 + k_{t,\perp}^2$ we can find

$$k_{t,\perp}^2 = k_t^2 - k_{t,\parallel}^2 \tag{34}$$
$$k_{t,\perp}^2 = \frac{n_2^2}{n_1^2}k^2 - k_{r,\perp} \tag{35}$$
$$k_{t,\perp}^2 = \omega^2\frac{n_2^2}{c^2}\left(1 - \frac{n_1^2}{n_2^2}\sin^2\theta_i\right)\,, \tag{36}$$

with $k_\parallel = k\sin\theta_i$. The last equation equals the dispersion relation (24) in the case of FTIR given above.

4 Evanescent Modes Are not Observable

Remarkable, evanescent modes like tunneling particles are not observable inside a barrier [21–23]. For instance, evanescent modes don't interact with an antenna as long as the system is not perturbed, i.e. the evanescent mode is not transformed back into a propagating electromagnetic wave. Evanescent modes like tunneling particles display some outstanding properties:

(1) The electric energy density u of the evanescent electric field E with its imaginary refractive index is negative:

$$u = \frac{1}{2}\epsilon E^2 \ < 0 \tag{37}$$
$$\epsilon \ = n^2 \ < 0. \tag{38}$$

In the case of particle tunneling we have a negative total kinetic W energy:

$$W = W_{\text{kin}} - U_0 \ < 0, \tag{39}$$

where W_{kin} and U_0 are the kinetic energy and the potential barrier height, respectively. Equation (37) is the quantum electrodynamic basis for the existence of evanescent waves. It has been shown by Ali [24] that virtual photons are those modes which do not satisfy the Einstein relation $W^2 \neq (\hbar k)^2c^2$.

(2) An evanescent field does not interact with real fields due to the imaginary wave number resulting in a refractive index mismatch. Fields can only transmit energy if for the reflection $R < 1$ holds. If n_1 represents the imaginary refractive index of an evanescent region and n_2 represents the refractive index of the dielectric medium then the square of the absolute value gives

$$R = \mid r \mid^2 = \frac{\mid n_2 - n_1 \mid^2}{\mid n_2 + n_1 \mid^2} \tag{40}$$

equals 1 and total reflection takes place.
In order to observe a particle in the barrier it must be localized within a distance of order $\Delta x \approx 1/\kappa$. Hence, its momentum Δp must be uncertain by

$$\Delta p > \hbar/\Delta x \approx \sqrt{2m(U_0 - W_{\text{kin}})} \tag{41}$$

The particle of energy W_{kin} can thus be located in the nonclassical region only if it is given an energy $U_0 - W_{\text{kin}}$, sufficient to raise it into the classically allowed region [22, 23].

(3) The quantization of evanescent modes by Carniglia and Mandel has shown that the locality condition is not fulfilled [25]. They figured out that the commutator of the field operator does not vanish for space-like separated points. This important point is discussed for EPR-correlations by Mittelstaedt [26].

5 Velocities, Delay Times, and Signals

We shortly define and discuss the velocities which can be associated to the various propagation phenomena of waves. *Remember, we are exclusively interested in the propagation of a cause, which is given by the signal velocity only.* We shall become aware that evanescent modes as well as tunneling wave packets are traveling independent of time. First the different quantities are made plausible by the sketch of two traveling wave packets displayed in Fig. 6. The wave packets are representative for voltage pulses of digital signals. The voltage oscillates with a frequency $\omega_0 \pm \Delta\omega$. The pulses begin and end gradually with time. In consequence a physical signal has no well defined front and front velocity. A well defined front and tail of a signal would presuppose an infinite frequency band width and then an infinite energy in consequence of $\hbar\omega$.

The phase velocity is given by the motion of a point stuck to the oscillations. The group velocity is given by the speed of the maximum of the packet, i.e. by the maximum of the pulse. The two velocities are equal in vacuum, but they may differ if traveling through interacting matter like glass or along a wave guide, for instance. The signal velocity is given by the speed of the envelope in order to measure the signal, which is in this example the indicated time duration at half pulse peak of the two pulses, so called half width. As seen by inspection of this figure, the signal and then the half width does not depend on its magnitude. In dispersive media with $n = f(\omega)$ group and signal velocities can be strongly different and the signal may be reshaped and lost its information, i.e. the cause. Such an example of pulse reshaping is displayed in Fig. 13. Essentially, here we are interested in the problem of causality, in cause and subsequent effect. A signal and then an effect can only be detected by its energy. In this respect signal and energy velocities are equal.

The notions on velocity and wave propagation are presented in many text books see Refs. [8, 11, 12], for instance.

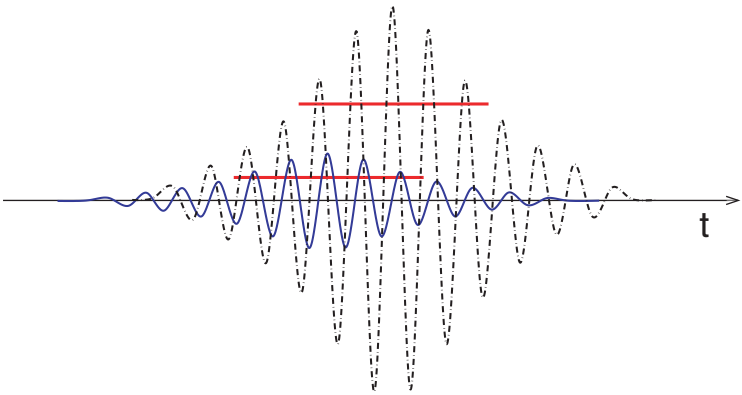

Fig. 6. Sketch of the oscillations of two wave packets (i.e. pulses) vs time. The larger packet has traveled slower than the attenuated one. The horizontal bars indicate the half width of the packets, which do not depend on the packet's magnitude. The figure illustrates the gradually beginning of the packets. The forward tail of the smooth envelope may be described by the relation $(1 - \exp(-t/\tau))\sin(\omega t)$ for instance, where τ is a time constant

5.1 Phase Velocity

Generally the phase velocity can be described by $\phi(\mathbf{x}, t) = Ae^{iS(\mathbf{x},t)}$, where $S(\mathbf{x}, t)$ is the phase of the wave and A its constant amplitude. The phase velocity is the speed related to the trajectory defined by the condition that the phase $S(\mathbf{x}, t)$ is constant, $S(\mathbf{x}, t) = const$. This condition relates $\mathbf{x}$ and t. From

$$0 = dS(\mathbf{x}, t) = \boldsymbol{\nabla} S \cdot d\mathbf{x} + \frac{\partial S}{\partial t} dt \tag{42}$$

and the definitions of the wave vector and the angular velocity

$$\mathbf{k} := -\boldsymbol{\nabla} S\,, \qquad \omega := \frac{\partial S}{\partial t} \tag{43}$$

we immediately obtain $\mathbf{k} \cdot \mathbf{v} = \omega$, where $\mathbf{v}_{\text{phase}} = d\mathbf{x}/dt$. With the dispersion relation $\omega = ck/n$ we obtain

$$\mathbf{k} \cdot \mathbf{v}_{\text{phase}} = \frac{c}{n(\omega)} k \tag{44}$$

or

$$v_{\text{phase,k}} = \frac{c}{n(\omega)}\,, \tag{45}$$

where $v_{\text{phase,k}}$ is the component of $\mathbf{v}_{\text{phase}}$ parallel to $\mathbf{k}$.

5.2 Group Velocity

The group velocity describes the velocity of the modulation of a harmonic traveling wave or of the peak of a wave packet. It is defined by

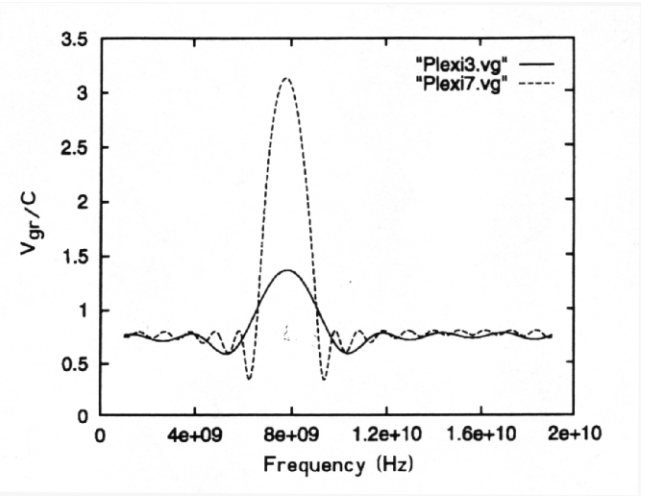

Fig. 7. Calculated group velocity vs frequency for two multiple layer structures as follows from (46) and Fig. 5

$$\mathbf{v}_{\text{group}} = \boldsymbol{\nabla}_k \omega(\mathbf{k})\,, \tag{46}$$

and represents the first term of a Taylor series of the modulation velocity. In vacuum, the group velocity equals c. See Fig. 7 for the group velocity in the case of a photonic lattice.

The group velocity can be rewritten as

$$v_{\text{group}} = \frac{d\omega}{dk} = \frac{c}{n(\omega) + \omega dn(\omega)/d\omega} \tag{47}$$

The last relation is interesting, as it elucidates the difference between the phase and the group velocity. It is the second term of the denominator, which distinguish the group from the phase velocity. For instance, in glass the group is about 2 % slower than the phase in the visible range of the spectrum.

We also have

$$v_{\text{group}} = \frac{x}{t_{\text{group}}} = \frac{x}{\partial S/\partial\omega}, \tag{48}$$

where $t_{\text{group}} = \partial S/\partial\omega$ is the group time delay or phase time. The phase shift is given by $\partial S = x\partial k$ in the region x considered. The group time delay represents the time delay of a maximum for traversing a distance as displayed in Fig. 13 for a strong dispersion. The case of a negligible dispersion shown in Figs. 1; 9. In the latter case the group time delay represents the time delay of a signal and of the energy.

5.3 Signal Velocity

A signal carries information which is a defined cause with a subsequent effect. For a simple example see digital signals shown in Fig. 8. Digital signals are given

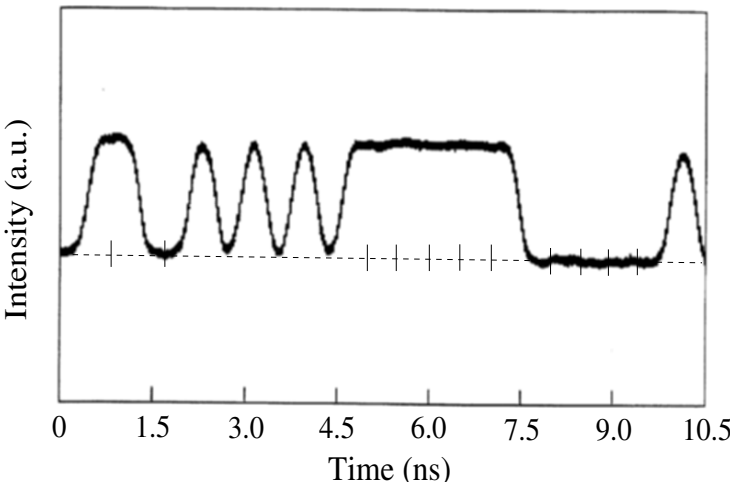

Fig. 8. Signals: Measured signal intensity in arbitrary units. The half width in units of 0.2 ns corresponds to the number of bits. From left to right: 1,1,0,0,1,0,1,0,1,0,1,1,1,1,1.... The infrared carrier frequency of the infrared signal is $2 \cdot 10^{14}$ Hz (wavelength 1.5 µm). The frequency-band-width of the signal is about $2 \cdot 10^{9}$ Hz corresponding to a relative frequency-band-width of 10^{-5} [17]

by their half width (the half width is the time span between the half power points, see e.g. Figs. 1; 6; 8; 9).

In general signals are characterized by their envelope, whether we are transmitting Morse signals, a word or a melody, always the complete envelope has to be measured, see [12], for instance. Therefore, the signal velocity in vacuum is identical to the group velocity in the case of negligible dispersion:

$$\mathbf{v}_{\text{signal}} \equiv \mathbf{v}_{\text{group}} \qquad (\text{in vacuum})\,. \tag{49}$$

Delay times and velocities are quantities depending only on the real part of the refractive index n' and on the derivative of the phase $S = 2\pi k_0 n' x$. In the case of evanescent modes or tunneling with a purely imaginary refractive index n'' the phase S is constant. *Thus according to (48) the group time delay becomes* $\rightarrow$ *0 and the group velocity* $\rightarrow \infty$. There is measured a phase shift and thus a short delay time corresponding to about one oscillation time of the signal in tunneling. This scattering time occurs at the front boundary and not inside the evanescent region nor inside a potential barrier. In the case of microwave pulses this time is about 100 ps and in the infrared case of glass fiber communication about 5 fs [13, 15], see also the data displayed in Fig. 5 and its interpretation. As this scattering time is independent of barrier length for opaque barriers with $\kappa x \geq 1$ (the so called Hartman effect) the effective group velocity (48) increases with barrier length [16]. This behavior is illustrated below in Figs. 5; 7.

The lack of phase shift means a zero-time barrier traversal of evanescent modes according to the phase time approach of (48). Actually this zero time

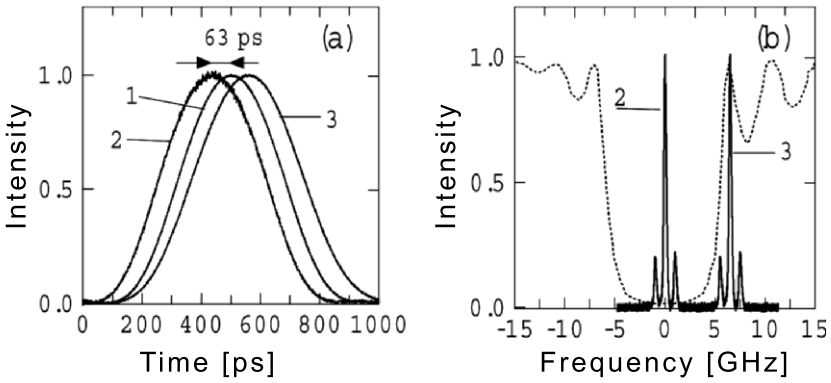

Fig. 9. (**a**) Measured propagation time of three digital signals and spectrum of the photonic lattice transmission [18]. Pulse trace 1 was recorded in vacuum. Pulse 2 traversed a photonic lattice in the center of the frequency band gap (see spectrum in part (**b**) of the figure), and pulse 3 was recorded for the pulse traveling through the fiber outside the forbidden band gap. The tunneling barrier was a photonic lattice of a quarter wavelength periodic dielectric hetero-structure fiber. The frequency zero point in part (b) corresponds to the infrared signal carrier frequency of $2 \cdot 10^{14}$ Hz and to the mid frequency of the forbidden frequency gap of the lattice

was measured in different experiments and the observed short barrier traversal time τ arises as scattering time at the barrier front boundary only [13, 15].

Infrared digital signals used in modern communication systems are displayed in Fig. 8. Such a single digit is tunneled and its velocity is compared with a vacuum and with a fiber traveled signal as shown in Fig. 9. Here Longhi et al. [18, 19] performed superluminal tunneling of infrared pulses over distances up to 50 mm at an infrared signal wavelength of 1.5 μm ($2 \cdot 10^{14}$ Hz). Results are presented in Fig. 9(Curve 1 luminal signal, 2 superluminal, 3 subluminal velocity). The frequency band width is $< 2 \cdot 10^9$ Hz. The measured velocity was $2\,c$ and the transmissivity of the barrier was 1.5%. The narrow band width of the signal is displayed in Fig. 9b. The superluminal signal pulse trace (2) has only evanescent frequency components around the mid frequency of the forbidden frequency gap of the photonic barrier.

5.4 The Front Velocity

As mentioned above the front velocity is an idealized notion and, thus, has no precise physical meaning. It is presupposing an infinite frequency band width of a signal. Its definition is given by

$$v_{\text{front}} = \lim_{\omega \to \infty} \frac{\omega}{k}\,. \tag{50}$$

Mathematically a discontinuity of the field under consideration or of one of its derivatives will propagate with the front velocity. The normal $(\omega, \mathbf{k})$ of the 3-dimensional hypersurface in 4-dimensional space-time where such discontinuities

may occur is defined by the characteristic equation

$$\omega^2 - \frac{c^2}{n^2}\mathbf{k}^2 = 0\,. \tag{51}$$

The velocity in configuration space related to the propagation of these singularities is then given by

$$\mathbf{v}_{\text{front}} = \boldsymbol{\nabla}_k \omega(\mathbf{k}) = \frac{c}{n}\widehat{\mathbf{k}}\,. \tag{52}$$

Therefore $v_{\text{front}} = c/n$. In vacuum, the front propagates with the velocity of light c. Though being a clear mathematical concept, it can be realized in physics only approximatively: Since a discontinuity is described by a Heaviside function (a function $H(x)$ which is zero for $x < 0$ and 1 for $x \geq 0$), the support of its Fourier transform is unbounded, that is, one needs waves with frequencies up to infinity in order to prepare a jump in the propagating field. This needs infinite energy which of course is not available. Therefore, since in reality only a finite range of frequency is available (frequency band limited signals), a jump in the propagating field cannot be created. However, there is no known *fundamental* limit for an upper energy bound (except perhaps the energy available in the universe). Therefore the front velocity is operationally not well defined and has no precise *physical* meaning [8, 12].

5.5 The Energy Velocity

Usually text books present the energy velocity by the relation ship

$$\mathbf{v}_{\text{energy}} = \mathbf{P}/u, \tag{53}$$

where

$$\mathbf{P} = \epsilon_0 c^2 \mathbf{E} \times \mathbf{B} \tag{54}$$

is the Poynting vector, E the electric field, B the magnetic field, and u is the energy density. The Poynting vector represents the energy flux and subtracts transmitted and reflected flux, whereas the scalar energy density adds both transmitted and reflected energy densities. This approach is then only correct in the case of no reflection and can not be applied for evanescent modes or tunneling, see e.g. [3]. The attenuation of evanescent modes is not due to dissipation but due to reflection. Equation (53) even can not be used to calculate the energy velocity in an open coaxial transmission line. Due to the impedance mismatch at the open end there takes place a strong reflection and (53) gives a too slow energy velocity for the energy loss at the end of the coaxial transmission line.

As already mentioned, we are interested in the *effect of a cause*. From this condition we can conclude that the energy velocity equals the signal velocity: A signal is received by an inelastic detection process. So it is the signal's energy which result in an defined effect.

6 Partial Reflection: An Experimental Method to Demonstrate Superluminal Signal Velocity of Evanescent Modes

Superluminal signal velocities were observed in different transmission and partial reflection experiments [5, 18–20]. The short tunneling and reflection times are equal. The result shows that the measured short time is spent at the barrier entrance. Inside a barrier the wave packet spends zero time. Transmission and reflection times are independent of barrier length as was calculated with the Schrödinger equation by Hartman and measured later [5, 13, 15, 27, 28]. This Hartman effect holds for opaque barriers with $\kappa x \geq 1$. The result demonstrate the nonlocal properties of evanescent modes and of the tunneling process as was shown by Carniglia and Mandel for instance [25].

A smart experimental set-up to measure both the transmission and the reflection times at the same time is sketched in Fig. 10. The distances of the reflected and of the transmitted beams differ only by the gap between the two prisms, i.e. the evanescent region (tunneling distance). *It was measured the same traveling time for both the reflected and the transmitted signals, obviously tunneling took place in zero-time [20].* The result was revisited by Stahlhofen [29] and was conjectured by quantum mechanical calculations for electron tunneling by Hartman and later by Low and Mende [27, 30]. The latter authors write that traversing a barrier appears to do so in *zero time*.

The reflection by a photonic lattice at a frequency of its forbidden band gap (see e.g. Fig. 9b) is measured and compared with the time crossing the same distance between two metallic mirrors. One mirror is positioned at the barrier

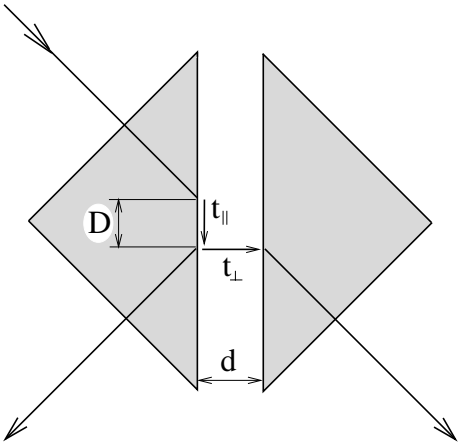

Fig. 10. Symmetrical FTIR set-up to measure both the reflection and the transmission time of a double prism, where $t_\perp$ is the time traversing the gap d and $t_\parallel$ is the time spent for traveling along the boundary of the first prism. The latter represents the time of the Goos–Hänchen shift [20]. The measured reflection time equals the transmission time resulting in a zero tunneling time $t_\perp = 0$

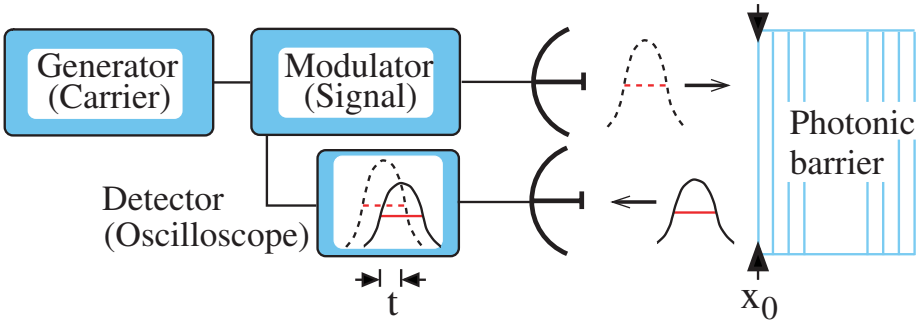

Fig. 11. Set-up to measure the time dependence of partial reflection at a photonic barrier with a digital pulse. The parabolic antenna on top of the illustration transmit digital pulses toward the barrier, the second one below receives the reflected signal. The time delay is measured with the oscilloscope

front side and the other one at the barrier back side. The set-up and the results are shown in Figs. 11, 12. The measured reflected time equals the time measured for the mirror's front position neglecting the mentioned short interaction time at the barrier front. The amazing result is that barrier height and barrier length

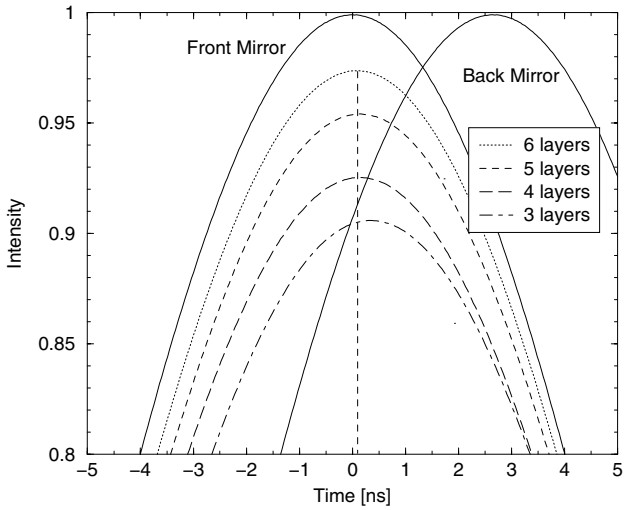

Fig. 12. Measured partial reflected microwave pulses vs time. Parameter is the barrier composition as illustrated in Fig. 11. The signal reflections from metal mirrors either substituting the barrier's front or back positions are displayed [28]. In this experiment the wavelength has been 3.28 cm and the barrier length was 40 cm. The number of lattice layers was reduced from 6 to 3 inside the resonant lattice structure illustrated in Fig. 11

are instantaneously displayed in the reflected signals as seen from inspection of Fig. 12.

The performance demonstrates that the reflected signal carries the information about barrier height and barrier length at the same time when the signal is reflected by the front mirror. The reflection time is independent of barrier length, the field spreading inside the barrier is instantaneous. The reflection amplitude decreases with decreasing barrier length but the reflection time is constant in the case of opaque barriers with $\kappa x \geq 1$.

7 Evanescent Modes a Near Field Phenomenon

According to many text books and review articles, superluminal signal velocities are violating Einstein causality, implying that cause and effect can be interchanged and that time machines known from science fiction can be designed [31–33]. Actually, it can be shown for frequency band *unlimited groups* that the front travels always at a velocity $\leq c$, and only the peak of the pulse has traveled with a superluminal velocity. As mentioned above such calculations were carried out by several authors, for example [34–36]. In this case the tunneled pulse is reshaped and its front has propagated at luminal velocity.

However, this approach does not describe physical signals as those signals displayed for instance in Figs. 1; 6; 8; 9. In this case the signal has gradually formed a front tail. A pulse reshaping did not happen and the envelope of the signal traveled at a superluminal velocity.

Pulse reshaping of a frequency band unlimited signal is displayed in Fig. 13. The half width of this artificial pulse with a discontinuous front step is significantly reduced compared with the original signal and only the pulse peak has traversed the barrier at superluminal velocity [34].

Frequently it is claimed that a tunneled small signal would not cross the front tail of the original signal, see for instance [34–36]. The argument is taken to prove that superluminal signal velocities are not allowed and do not occur. The frequency band limited digital signals presented in Figs. 1; 9 are crossing each other. This result is in consequence of the fact that these superluminal pulses contain only evanescent frequency components.

A physical signal can not be described by a Gauss function having an infinite frequency band. For a physical signal the relation [11, 37]

$$\Delta\nu \cdot \Delta t \geq 1, \tag{55}$$

holds, whith both $\Delta\nu$ and $\Delta t \ll \infty$. Such a pulse of field oscillations is sketched in Fig. 6. Actually, relation (55) is proportional to the information content of a signal as was shown by Shannon [37]. According to Fourier transform such a physical signal with both limited frequency band and time duration is not causal [12, 38]. On the other hand it is obvious that a physical signal has to be frequency band limited. Signals start gradually within a time span given by its frequency band width [8, 12].

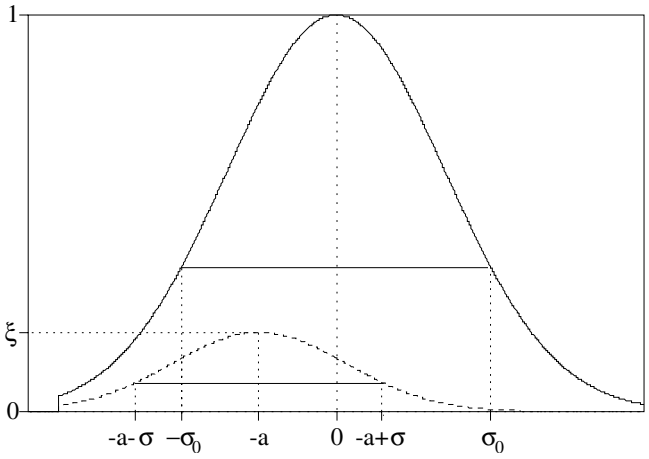

Fig. 13. Comparison of calculated intensity vs time of an airborne pulse (*solid line*) and the same tunneled pulse (*dotted line*) [34]. Both signals have a sharp step at the front and thus an infinite frequency bandwidth. The tunneled signal is reshaped and attenuated. Its maximum has traveled at superluminal velocity. Both fronts have traversed the same distance with speed c, ξ is the maximum of the tunneled pulse, a is the shift of the maximum, σ is the halfwidth of the tunneled signal, and σ_0 is the halfwidth of the airborn signal [34]. The halfwidths $\sigma \gg \sigma_0$ holds, i.e. the digital information is strongly reshaped

As the Gauss function does not describe a physical signal, mathematicians and engineers have developed a number of so called window functions [39]. They are limited in both frequency and time but can be quasi causal transformed from time to frequency domain and vice versa.

For example, physical digital signals are well described by the Kaiser-Bessel function for instance. This function is used in network analyzers describing the intensity vs time as well as the frequency band of physical signals. This function allows even a causal Fourier transform from time domain to frequency domain down to intensities at which the Johnson noise limits detectors finally, see (57, 58).

In Figs. 14 and 15 the Kaiser-Bessel function is plotted as a function of intensity I(t) vs time. The curves can be scaled to the data of the experiments displayed in Figs. 1 and 9.

The Kaiser–Bessel function – often called Kaiser–Bessel window as time duration and frequency spectrum are limited – is given

$$I(t) = \frac{I_0\left(\pi \Delta t \Delta\nu (1 - \sqrt{\frac{t}{\Delta t/2}})\right)}{I_0 \pi \Delta t \Delta\nu}, \tag{56}$$

where I_0, and $\pi \Delta t \Delta\nu$ are the zero-order modified Bessel function of the first kind, and the time-bandwidth product, respectively. $0 \leq |t| \leq \Delta t/2$, represents the investigated time interval.

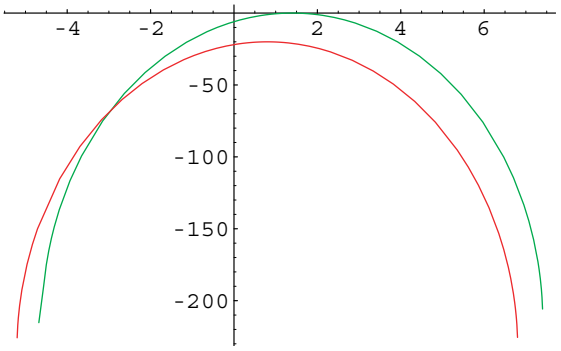

Fig. 14. Calculated pulse intensity of the Kaiser–Bessel function vs time in a.u.. The data can be scaled to the measured pulses displayed in Figs. 1; 8; 9. In the graph the tunneled signal is attenuated by −20 dB

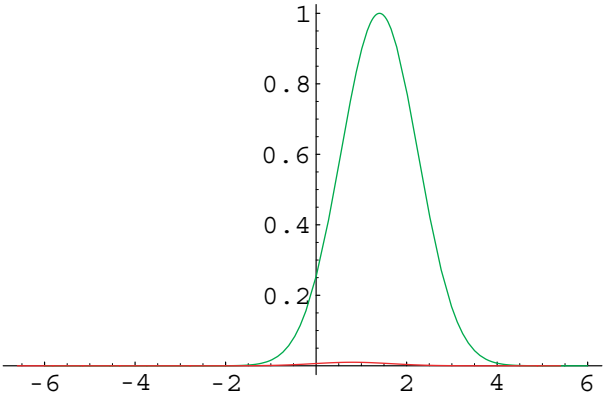

Fig. 15. The same data as shown in Fig. 14 in a semi-logarithmic plot. The ordinate is scaled in dB and the abscissa in a.u.

A signal can be detected only if its power is above the Johnson noise P_{JN}. The thermal noise was observed and measured by Johnson in 1928 and is theoretically elaborated by the Nyquist Theorem, see for instance [40]. The theorem is of great importance in experimental physics and electronics. It is concerned with the spontaneous thermal fluctuations of voltage across an electric circuit element. The theorem gives a quantitative expression for thermal noise power generated by a resistor in thermal equilibrium:

$$P_{\mathrm{JN}} = kT\Delta f, \tag{57}$$

This relation yields a classical estimate for the near field extension of evanescent modes. The power $P(x)$ of a signal, i.e. of a defined effect has to be detected. Then superluminal signal propagation is limited by the relationship, which gives the minimum tunneled signal power:

$$P(x) = P_0 e^{-2\kappa x} \geq kT\Delta f, \tag{58}$$

where P_0 is the incident power of the evanescent mode, κ is the imaginary wave number of the evanescent mode, x the length of the evanescent region, k the Boltzmann constant, T the temperature, and Δf the frequency range of the signal. For example an infrared signal source of 1 mW power, a carrier frequency of $2 \cdot 10^{14}$ Hz (1.5 µm wavelength), and an imaginary wave number in the barrier $\kappa = 115\,\mathrm{m}^{-1}$ at a temperature of $T = 300\,\mathrm{K}$. Thus the Johnson noise with $\approx 1\,\mu\mathrm{W}$ limits a detectable near field up to 0.03 m, corresponding to about 20000 wavelengths of this infrared digital signal and this special photonic barrier. In the above introduced microwave experiments the near field was limited to less than a hundred wave lengths.

8 Superluminal Signals Do not Violate Primitive Causality

Does the measured superluminal signal velocity violate the principle of causality? The line of arguments showing how to manipulate the past in the case of superluminal signal velocities is illustrated in Fig. 16. There are displayed two frames of reference. In the first one lottery numbers are presented as points on the time coordinate with zero time duration. At $t = 0$ the counters are closed. Mary (A) sends the lottery numbers to her girl friend Susan (B) with a signal velocity of $4; c$. Susan, moving in the second inertial system at a relative speed of 0.75 c, sends the numbers back at a speed of 2 c, to arrive in the first system of Mary at $t = -1$ s, thus in time to deliver the correct lottery numbers before the counters close at $t = 0$.

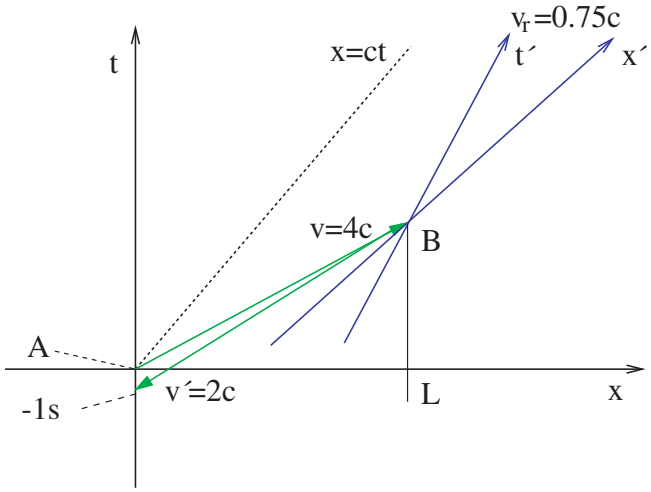

Fig. 16. Coordinates of two inertial observers **A** $(0, 0)$ and **B** with $O(x, t)$ and $O'(x', t')$ moving with a relative velocity of 0.75 c. The distance L between **A** and **B** is 2 000 000 km. **A** makes use of a signal velocity $v_s = 4\ c$ and **B** makes use of $v'_s = 2c$ (in the sketch is $v \equiv v_s$). The numbers in the example are chosen arbitrarily. The signal returns -1 s in the past in **A**

The time shift of a point on the time axis of reference system A into the past is given by the relation, [32, 41],

$$t_A = -\frac{L}{c} \cdot \frac{(v_r - c^2/v_s - c^2/v'_s + c^2 v_r/v_s v'_s)}{(c - c v_r/v'_s)}, \tag{59}$$

where L is the transmission length of the signal, v_r is the velocity between the two inertial systems A and B. The condition for the change of chronological order is $t_A < 0$, the time shift between the systems A and B. This interpretation assumes, however, a signal to be of zero time neglecting its temporal width.

Several tunneling experiments have revealed superluminal signal velocity in tunneling photonic barriers [5]. Nevertheless, the principle of causality has not been violated as will be explained in the following.

In the example with the lottery data, the signal was assumed to be a point in space-time. However, a physical signal has a finite duration like the pulses sketched along the time axis in Fig. 17.

The general relationship for the bandwidth-time interval product of a signal, i.e. a packet of oscillations is given by (55). A zero time duration of a signal would require an infinite frequency bandwidth.

Taking into consideration the dispersion of the transmission of tunneling barriers, the frequency band of a signal has to be narrow in order to suppress non superluminal frequency components and thus pulse reshaping.

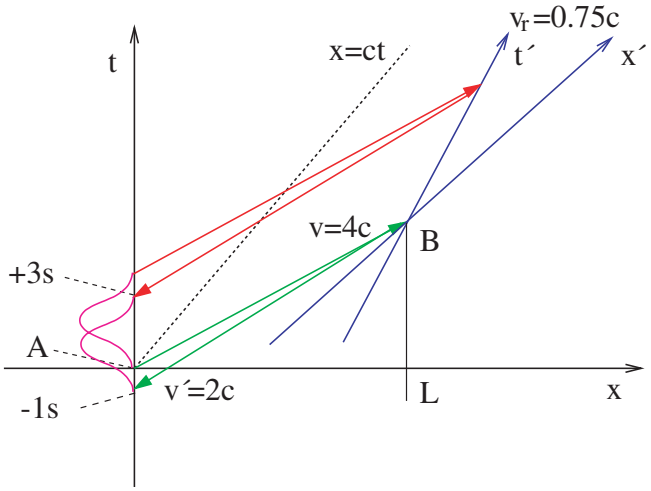

Fig. 17. In contrast to Fig. 16 the pulse-like signal has now a finite duration of 4 s. This data is used for a clear demonstration of the effect. In all superluminal experiments, the signal length is long compared with the measured negative time shift. In this sketch the signal envelope ends in the future with 3 s (in the sketch is $v \equiv v_s$)

Assuming a signal duration of 4 s the complete information is obtained with superluminal signal velocity at 3 s at a positive time as illustrated in Fig. 17.

The compulsory finite duration of all signals is the reason that a superluminal velocity does not violate the principle of causality. A shorter signal with the same information content would have an equivalently broader frequency bandwidth, compare (55). As a consequence, an increase of v_s or v_s' cannot violate the principle of causality.

For instance, the dispersion relation of FTIR (24) elucidate this universal behavior: Assuming a wavelength $\lambda_0 = c/\nu$, a tunneling time $\tau = T = 1/\nu$, and a tunneling gap between the prisms $d = j\,\lambda_0$ $(j = 1, 2, 3, \ldots)$ the superluminal signal velocity is $v_s = j\,c$, (remember the tunneling time is independent of barrier length). However, with increasing v_s the bandwidth $\Delta\nu$ (that is the tolerated imaginary wave number width $\Delta\kappa$) of the signal decreases $\propto 1/d$ in order to guarantee the same amplitude distribution of all frequency components of the signal. In spite of an increasing superluminal signal velocity $v_s \to \infty$ the general causality can not be violated because the signal time duration increases analogously $\Delta t \to \infty$, see (55).

9 Summary

Evanescent modes and tunneling show amazing properties to which we are not used to from classical physics. The tunneling time is short and arises at the barrier front as scattering time. This time equals approximately the reciprocal frequency of the carrier frequency or of the wave packet energy divided by the Planck constant h [13, 15]. Inside a barrier the wave packet does spent zero time [5, 30]. This property results in superluminal signal and energy velocities, as a signal is detected by its energy, i.e. by photons or other field quanta like phonons. The detector receives the tunneled signal earlier than the signal, which traveled the same distance in vacuum as demonstrated in Figs. 1, 9, 12. Evanescent fields like tunneling particles are not observable [22, 23, 25, 42–44].

Another consequence of the frequency band limitation of signals is, if they have only evanescent mode components, as shown for instance in Fig. 9b signal trace (2), they can violate relativistic causality, which claims that signal and energy velocities have to be $\leq c$.

As explained in Sec. evanescent modes and the tunneling process are near field effects. They are roughly limited to the order of the signal length in propagating in vacuum.

In the review on *The quantum mechanical tunnelling time problem - revisited* by Collins et al. [45], the following statement has been made on the much ado about superluminal velocity: *the phase-time-result originally obtained by Wigner and by Hartman is the best expression to use for a wide parameter range of barriers, energies and wave packets.* The experimental results of photonic tunneling have confirmed this statement [5]. In spite of so much arguing about violation of Einstein causality [4, 33, 36, 46, 47], all the properties introduced above are useful for novel devices, for both photonics and electronics [48].

Acknowledgement

I like to thank Claus Lämmerzahl and Alfons Stahlhofen for stimulating and elucidating discussions. The technical advice and support by Horst Aichmann, Astrid Haibel, Harald Spieker, Ralf Vetter, and Igor Drozdov are gratefully acknowledged.

References

1. A. Enders and G. Nimtz, J. Phys. I, France **2**, 1693 (1992)
2. V. Olkhovsky and E. Recami, Phys. Rep. **214**, 339 (1992); E. Recami, Int. J. of Modern Physics, **A 15**, 2793 (2000); V. Olkhovsky, E. Recami, J. Jakiel, Phys. Rep. **398**, 133 (2004).
3. G. Nimtz and W. Heitmann, Progr. Quant. Electr. **21**, 81 (1997).
4. R. Chiao and A. Steinberg, Progress in Optics **XXXVII**, 345 (1997).
5. G. Nimtz, Prog. Quantum Electronics **27**, 417 (2003).
6. R.P. Feynman, R.B. Leighton, and M. Sands, The Feyman Lectures on Physics, **II** 33–12, Addison–Wesley, Reading (1964).
7. G. Nimtz, A. Enders, and H. Spieker, J. Phys. I, France **4**, 565 (1994).
8. L. Brillouin, Wave propagation and group velocity, Academic Press, New York (1960).
9. L. Wang, A. Kuzmich, and A. Dogariu, Nature **406**, 277 (2000).
10. D. Bowmeester, J. Pan, K. Mattle, M. Eibl, H. Weinfurter, and A. Zeilinger, Nature, **390**, 575 (1997).
11. Berkeley physics course, **3**, Chap. 6, McGraw-Hill , New York and London (1968).
12. A. Papoulis, The Fourier Integral And Its Applications, McGraw-Hill, New York, Secs. 7.5 and 7.6 (1962).
13. S. Esposito, Phys. Rev. E **64**, 026609 (2001).
14. J.M. Bendickson, J.P. Dowling, and M. Scalora, Phys. Rev. E **53**, 4107 (1996).
15. A. Haibel and G. Nimtz, Ann. Phys. (Leipzig) **10**, 707 (2001).
16. A. Enders and G. Nimtz, Phys. Rev. E **48**, 632 (1994).
17. E. Desurvivre, Scientific American **266** January, 96(1992).
18. S. Longhi, M. Marano, P. Laporta, and M. Belmonte, Phys. Rev. E **64**, 055602 (2001).
19. S. Longhi, P. Laporta, M. Belmonte, and E. Recami, Phys. Rev. E **65**, 046610 (2002).
20. A. Haibel, G. Nimtz, and A.A. Stahlhofen, Phys. Rev. **E 63**, 047601 (2001).
21. J.P. Fillard, Near field optics and nanoscopy, Worls scientific, Singapore (1997).
22. E. Merzbacher, *Quantum Mechanics*, 2nd edition, John Wiley & Sons, New York (1970).
23. S. Gasiorowicz, Quantum Physics, John Wiley & Sons, New York (1996).
24. S.T. Ali, Phys. Rev. B **7**, 1668 (1973).
25. C.K. Carniglia and L. Mandel, Phys. Rev. D **3**, 280 (1971).
26. P. Mittelstaedt, Ann. Phys. (Leipzig) **7**, 710 (1998).
27. Th. Hartman, J. Appl. Phys. **33**, 3427 (1962).
28. G. Nimtz, A. Haibel and R.-M. Vetter, Phys. Rev. E **66**, 037602 (2002).
29. A.A. Stahlhofen, Phys. Rev. A **62**, 12112 (2000).
30. F.E. Low and P.F. Mende, Ann. Phys. NY **210**, 380 (1991).

31. M. Fayngold, Special Relativity and Motions Faster than Light, Wiley-VCH, Weinheim, 219–223 (2002).
32. R. Sexl und H. Schmidt, Raum-Zeit-Relativität, vieweg studium, Braunschweig (1978).
33. R.U. Sexl and H.K. Urbantke, Relativity, Groups, Particles, Springer, Wien, NewYork (2001).
34. Th. Emig, Phys. Rev. **E 54**, 5780 (1996).
35. G. Diener, Phys. Letters A, **235**, 118 (1997).
36. H. Goenner, Ann. Phys. (Leipzig), **7**, 774 (1998).
37. C.E. Shannon, Bell Sys. Tech. J., **27**, 379, and 623 (1948).
38. D.C. Champeney, Fourier Transforms and their Physical Applications, Academic Press, London and New York (1973).
39. F.J. Harris, Proc. IEEE, **66**, 51 (1978).
40. C. Kittel, Thermal Physics, John Wiley & Sons, New York (1968), pp. 402–405.
41. P. Mittelstaedt, Eur. Phys. J, **B 13**, 353 (2000).
42. G. Nimtz, Gen. Rel. Grav. **31**, 737 (1999); G. Nimtz, Ann. Phys. (Leipzig), **7**, 618 (1998).
43. F. de Fornel, Springer Series in Optical Sciences, **73**, Springer, Berlin (2001).
44. O. Bryngdahl, Progress in Optics, **11**, 167 (1973).
45. S. Collins, D. Lowe and J. Barker, J. Phys. C, **20**, 6213 (1987).
46. M. Büttiker and H. Thomas, Superlattices and Microstructures, **23**, 781 (1998).
47. M. Stenner, D. Gauthier, and M. Neifeld, Nature, **425**, 695 (2003); G. Nimtz and Stenner et al., Nature, **6 May**, (2004).
48. G. Nimtz, IEEE Journal of selected topics in quantum electronics, **9**, 79 (2003).